J Electroceram (2008) 21:672–676
DOI 10.1007/s10832-007-9269-1

Properties of (001)-textured $Pb(Mg_{1/3}Nb_{2/3})O_3$–$PbTiO_3$ thin films

Wen Gong · Xiangcheng Chu · Jing-Feng Li · Longtu Li

Published online: 21 August 2007
© Springer Science + Business Media, LLC 2007

Abstract Relaxor ferroelectric $Pb(Mg_{1/3}Nb_{2/3})O_3$–$PbTiO_3$ (PMN–PT) thin films with [001] preferential orientation were deposited on platinized silicon wafers by a sol–gel method, in which a PbO seeding layer was involved. The influences of annealing temperature on the crystal phase, microstructure, and electrical properties of the PMN–PT films were investigated. Pyrochlore-free perovskite PMN–PT films could be formed on PbO-seeded Pt(111)/Ti/SiO_2/Si wafers at 800 °C, which was also the optimal annealing temperature for endowing the film with the best ferroelectric and dielectric properties. The enhanced properties were attributed to the improved crystallinity and microstructure. The leakage behaviors of the PMN–PT films annealed at different temperatures were also measured and discussed.

Keywords Ferroelectric · Dielectric · Sol–gel · Thin films · PMN–PT

1 Introduction

Lead-base ferroelectric thin films such as $PbTiO_3$ (PT), Pb(Zr,Ti)O_3 (PZT) and $Pb(Mg_{1/3}Nb_{2/3})O_3$–$PbTiO_3$ (PMN–PT) are very interesting materials for applications in electronic devices and micro-electro-mechanical systems (MEMS) [1–3]. Due to its high dielectric constant and piezoelectric coefficient, PMN–PT system is a promising candidate for integration on silicon substrates in MEMS microactuators [4, 5]. Compared with the extensively studied PZT system, there are fewer reports on PMN–PT thin films because of its trend of forming in pyrochlore rather than perovskite. The later needs a higher processing temperature and more accurate stoichiometry. To suppress the formation of pyrochlore phases, Fan et al. use a PbO over coat to compensate the lead loss of PMN–PT films [6]. The sol–gel method enables us to prepare a film with a homogeneous thickness and accurate stoichiometry. In our previous study [7], a PbO seeding layer was introduced in the spin-coating process to control the texture of PMN–PT thin films. We found that, with the presence of the PbO seeding layer, not only the prepared PMN–PT thin films were absolutely (001)-textured, but also the annealing temperature was reduced. As revealed by our recent studies, the electric properties of PZT films greatly depend on the crystal orientation. However, compared with PZT films, the properties of relaxor ferroelectric PMN–PT films are little known. In this study, we investigated the dielectric and ferroelectric properties of textured PMN–PT thin films, with an emphasis placed on the microstructure of the PMN–PT films resulting from different annealing temperatures.

2 Experimental procedure

In this study, the substrates were widely used Pt(111)/Ti/SiO_2/Si wafers, whose Pt electrode of 180 nm thick was deposited on a thermally oxidized silicon layer by RF magnetron sputtering, with Ti (about 10 nm) as an adhesive layer. The precursor solution with a composition near the morphotropic phase boundary ($[Pb(Mg_{1/3}Nb_{2/3})O_3]_{0.7}$–$[PbTiO_3]_{0.3}$) was prepared and diluted to 0.5 M. The precursor solution contained 30 mol% excess lead oxide addition as referred to the nominal PMN–PT composition, which was required to compensate for the Pb loss and promote the perovskite phase formation. Lead-containing organic solution (0.02 M) was prepared for the lead oxide

W. Gong · X. Chu · J.-F. Li (✉) · L. Li
State Key Laboratory of New Ceramics and Fine Processing,
Department of Materials Science and Engineering,
Tsinghua University,
Beijing 100084, People's Republic of China
e-mail: jingfeng@mail.tsinghua.edu.cn

seeding layer using the similar procedure. PMN–PT films were deposited onto the substrates using the spin coating method, which was described in detail in the work of Suzuki et al. and Kighelman et al. [8, 9]. Prior to the deposition of a PMN–PT layer, the substrate was spin-coated by the prepared lead organic solution and annealed at 500 °C for 2 min to form a lead oxide seeding layer on the bare platinum electrode. Subsequently, a PMN–PT gel layer was deposited on the lead oxide layer by the spin-coating method for 5 times, each followed by pyrolysis at 450 °C. Additional annealing treatment was conducted for 2 min at temperatures ranging from 700 to 800 °C by using a rapid thermal processing (RTP) furnace in an oxygen atmosphere for densification and crystallization.

The crystalline structure of the PMN–PT films was analyzed by X-ray diffraction (XRD, Rigaku, D/max-RB) with Cu–Kα radiation. The surface morphology and cross-sectional microstructure of the films were observed by using a field-emission scanning electron microscope (FE–SEM, Hitachi, S4300) and a transmission electron microscope (TEM, JEOL, 2010F), respectively. The chemical composition depth profile of the films was determined by Auger electron spectroscopy (AES, Perkin–Elmer, PHI-6001/SAM). Top electrodes of platinum, approximately 0.1 μm in thickness and 0.7 mm in diameter, were sputtered onto the top surfaces of the prepared PMN–PT films for relevant electrical measurements. The ferroelectric and dielectric properties were characterized using a ferroelectric test module (aixACCT, Analyzer 2000 FE).

3 Experimental results

Figure 1 shows the XRD patterns of the prepared PMN–PT films annealed at different temperatures. As shown in Fig. 1, these films were grown in pseudo-perovskite phase with [001] texture. When annealed above 700 °C, the amorphous film transformed to the pseudo-perovskite phase with residual pyrochlore phase detected at about 29° (2θ). This peak intensity become weaker but remains as the annealing temperature was increased up to 750 °C. As annealed at 800 °C, the PMN–PT film shows a pronounced [001] peak with a small hump at 30.8°, implying the secondary nucleation ([110]-oriented crystals) in the film. In comparison with the films annealed at relatively lower temperatures, the [001] peak of the PMN–PT film annealed at 800 °C shows higher relative intensity, indicating an enhanced degree of crystallinity and texture. In the case of 850 °C, there is no apparent change from the film annealed at 800 °C. We found that annealing at 800 °C for 2 min enhanced the evolution of pseudo-perovskite phase and suppression of pyrochlore phase. The presence of lead oxide seeding layer was believed to play a key role in phase evolution of PMN–PT. More discussion on the effect of the lead oxide seeding layer was detailed in the work of Gong et al. [7].

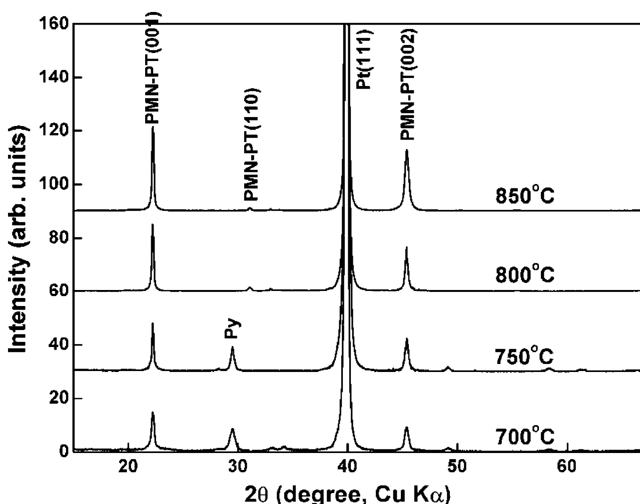

Fig. 1 The XRD patterns of PMN–PT films on Pt(111)/Ti/SiO_2/Si substrates, annealed at various temperatures. *Py* denotes pyrochlore phase

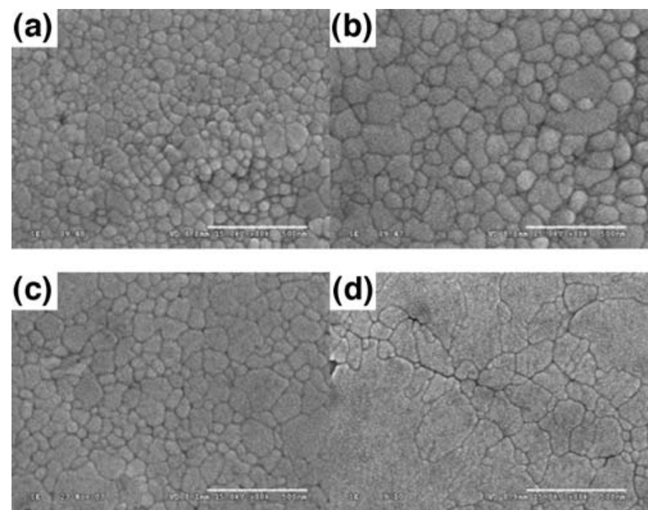

Fig. 2 SEM micrographs of the surface morphology of PMN–PT films annealed at different temperatures: (**a**) 700 °C, (**b**) 750 °C, (**c**) 800 °C and (**d**) 850 °C. The *bars* represent 500 nm

Figure 2 shows a series of SEM images of the surface morphology of the films annealed at different temperatures ranging from 700 to 850 °C. Dense and crack-free microstructures were obtained for all the temperatures investigated. The grains grow from 50–100 nm to near 500 nm in diameter, when the annealing temperature was raised from 700 to 850 °C. In addition, the grain size became non-uniform at higher temperature, as shown in Fig. 2(d). However, it was confirmed that the surface roughness of the film annealed at higher temperature was improved.

Figure 3 shows a TEM micrograph corresponding to the cross section of the PMN–PT film annealed at 800 °C for 2 min and the inset is the selected area electron diffraction (SAED) pattern near the PMN–PT/Pt interface. In view of

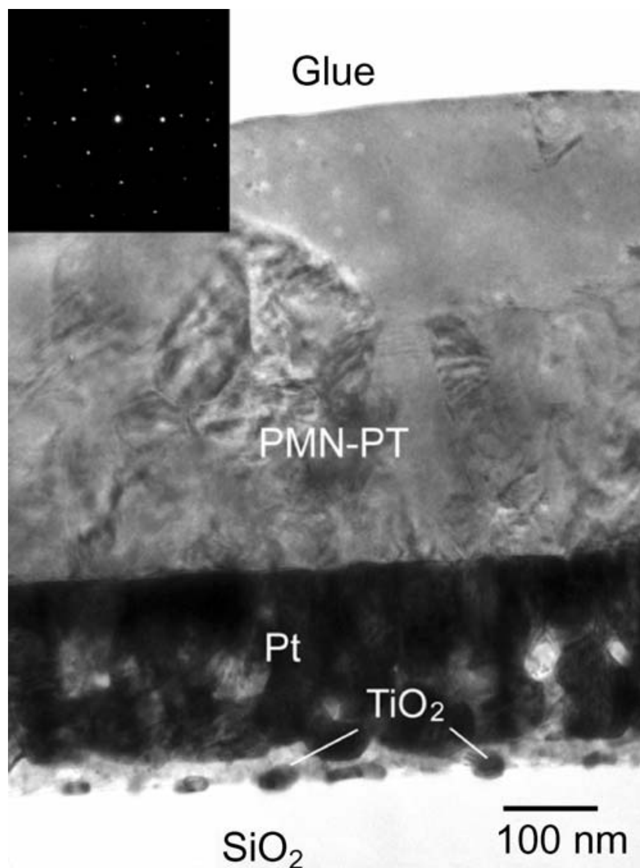

Fig. 3 TEM micrograph of transverse section of the PMN–PT film annealed at 800 °C for 2 min. The *inset* is the SAED pattern near the PMN–PT/Pt interface

the lead oxide layer, the film/electrode interface was carefully examined by TEM to investigate the state of the lead oxide seeds. As shown in Fig. 3, there is a sharp interface between the PMN–PT film and the platinum electrode. In addition, the SAED pattern from this region shows that there is no secondary phase. Although the platinum electrode was pre-coated with a lead oxide layer, the TEM observation indicates no secondary phase near the interface. Meanwhile, the depth profile using AES (Fig. 4(a)) also confirmed that there was no lead-rich layer near the film/electrode interface for the film annealed at 800 °C. The very limited amount of lead oxide seeds could be dissolved into the overlaid film when the annealing temperature was sufficiently high. However, the lead-concentration at the interface was somewhat high for the film annealed at a relatively lower temperature, as shown in Fig. 4(b), probably because the annealing temperature was not high enough, or the annealing time was not long enough for the lead diffusion into the films.

The residual pyrochlore phase and lead-rich layer were considered to greatly affect the ferroelectric and dielectric properties of the prepared PMN–PT films. A comparison of the hysteresis loops between the PMN–PT films annealed at 750 °C and 800 °C is presented in Fig. 5. In both cases, the polycrystalline PMN–PT films showed a typical relaxor ferroelectric hysteresis loop. Although the annealing temperature was as low as 750 °C, the well-behaved hysteresis loop was observed. However, the saturation polarization value varied significantly even for the 50 °C difference of annealing temperature. For the PMN–PT film annealed at 800 °C, the maximum value of polarization is 34 $\mu C/cm^2$ at an electrical field of 200 kV/cm. The coercive electrical field slightly decreased with increasing annealing temperature.

The leakage behavior of the prepared PMN–PT films was found to greatly depend on the annealing temperature. The measured leakage properties are summarized in Fig. 6. Although the films annealed at relatively lower temperatures consist of a small portion of pyrochlore phase as shown in Fig. 1, the leakage current density was restricted to a low level. On the contrary, for the PMN–PT films annealed at a

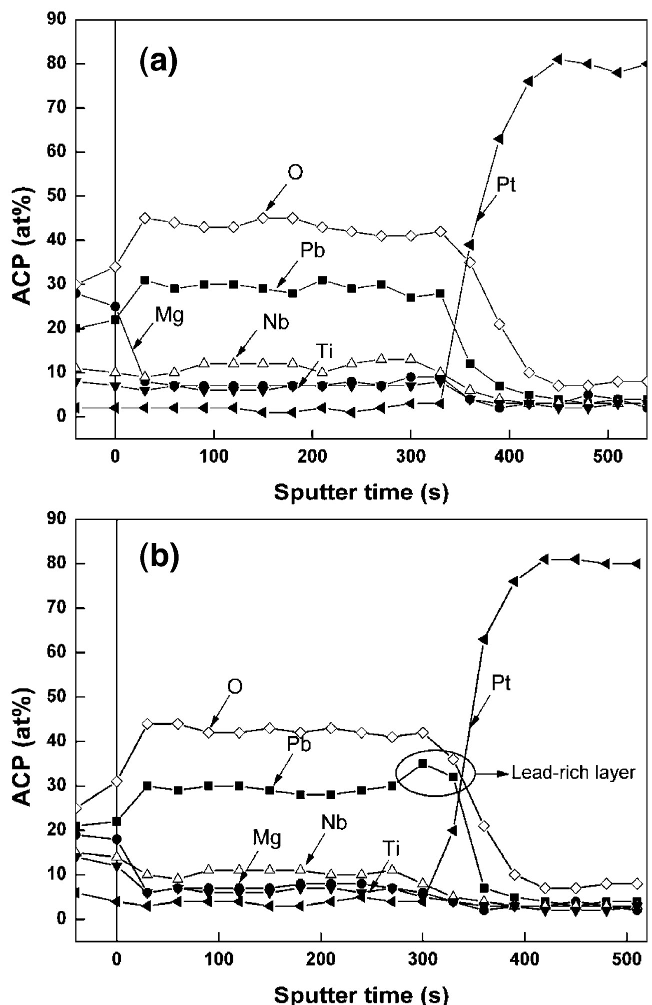

Fig. 4 Depth profiles of the PMN–PT films annealed at (**a**) 800 °C and (**b**) 750 °C

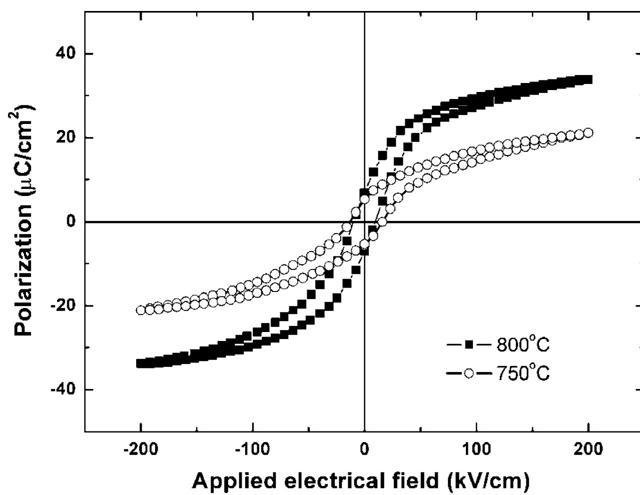

Fig. 5 *P–E* hysteresis loops of the prepared PMN–PT films annealed at 750 and 800 °C, respectively

high temperature, especially for 850 °C, the current leakage increased by two order of magnitude as compared with that annealed at 800 °C.

The relative dielectric constant and loss factor were also measured as a function of annealing temperature. In agreement with the best ferroelectricity in the PMN–PT film annealed at 800 °C, the maximum of relative dielectric constant (ε_r=1290) is also obtained at 800 °C, with a corresponding loss factor of 0.17. The residual pyrochlore accounts for the low dielectric properties of the PMN–PT

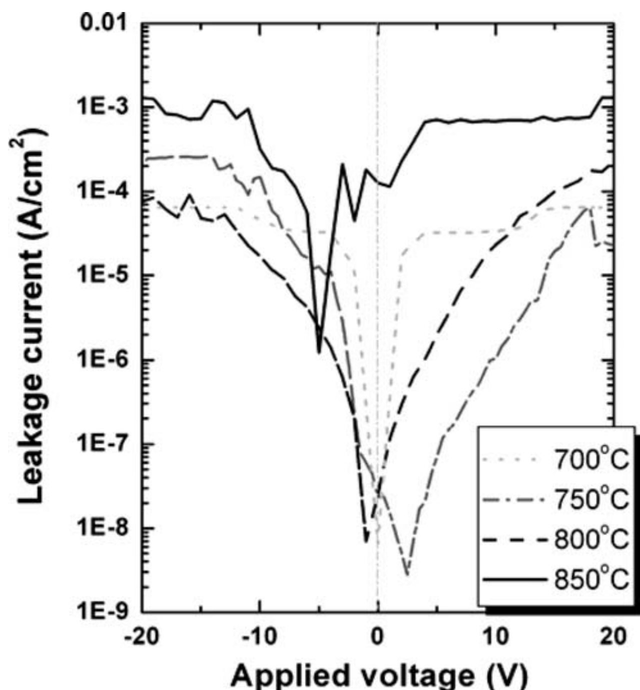

Fig. 6 Logarithmic plot of the median current intensity (J_m) versus applied voltage for PMN–PT films annealed at different temperatures

films annealed at 700 and 750 °C. The dielectric constant decreases slightly when the annealing temperature increases from 800 to 850 °C. It is considered that the perovskite phase would be fully formed at 800 °C, resulting in the maximum of the dielectric property, which is larger than that of PZT films reported in our previous work [10]. As the annealing temperature was raised to 850°C, the lead loss at the surface region occurred, reducing the overall dielectric properties of the whole film.

4 Discussion

The PMN–PT film annealed at 750 °C shows a certain amount of residual pyrochlore, which is a paraelectric phase. When the annealing temperature was increased by 50 °C, the *P–E* hysteresis behavior of the films was improved, showing a larger saturation polarization and smaller coercive field. Such a change can be attributed to the formation of nearly single-phase perovskite films with improved crystallization at a high annealing temperature. Furthermore, the variation in grain size is assumed to be partially responsible for the enhanced ferroelectric properties as well. Since the reversible domain switching is pinned in fine grains, a higher external electrical field is required to polarize the PMN–PT film annealed at a relatively low temperature. The measured *P–E* loops for these PMN–PT films are therefore influenced by a combination of these effects.

The annealing treatment affects the local elemental distribution and microstructure across the interface. Es-Souni et al. [11] put forward a "Matterhorn picture" model, in which a thin layer near the metal electrodes with a large concentration of trapped charges and large electrical field was proposed. In the case of the PMN–PT film annealed at a relatively low temperature, the lead-rich layer near the bottom electrode has much in common with that model. Consequently, it is considered that the conductivity mechanism is primarily interface-controlled. Boerasu et al. [12] demonstrated that, for metal/film/metal structure, Pb$(Zr_{0.65}Ti_{0.35})O_3$ thin films obey the "1/4 law", which was described using the following formula:

$$\ln J_m = \text{const} + b(V + V_{bi})^{1/4} \tag{1}$$

where b is related to the acceptor concentration and V_{bi} is the build-in voltage (determined by *C–V* curves). In this investigation, we found that the "1/4 law" was also suitable for characteristics of the leakage behavior in PMN–PT thin films, indicating that the Schottky emission model [13] is qualitatively correct to interpret the conductivity mechanism. That is, the conductivity is controlled by interface phenomena.

5 Conclusion

(001)-textured PMN–PT films were prepared by sol–gel process, and the influences of annealing temperature on the ferroelectric and dielectric properties were investigated. The experimental results enabled us to draw the following conclusions:

(1) The lead oxide seeding layer on the surface of Pt(111)/ Ti/SiO_2/Si substrates deduced the (001) preferential growth of the overlaid PMN–PT films at a reduced annealing temperature.
(2) Almost single-phase perovskite PMN–PT films were obtained for the annealing at 800 °C, resulting in a sharp interface between the PMN–PT film and the platinum electrode. However, as the annealing temperature was not sufficiently high, there was a considerable amount of residual pyrochlore phase in the film and a thin lead-rich layer at the film/electrode interface, even though the annealing temperature was lower by 50 °C than the optimal value (800 °C).
(3) The ferroelectric and dielectric properties were sensitive to the film microstructure and the characteristic of interfaces. Because of the residual pyrochlore and lead-rich layer, the PMN–PT films annealed at relatively lower temperatures exhibited lower ferroelectric and dielectric properties. Furthermore, the lead-rich thin layer near the film/electrode interface great affected the leakage current behavior. In this case, the Schottky emission model was reasonable as an interpretation for the results for the PMN–PT films.

Acknowledgements This work was supported by the Ministry of Science and Technology of China (grant no. 2002CB613306), the National Natural Science Foundation (Grants Nos. 50325207, 50621201 and 50672040), and the Hi-Tech Research & Development Program of China (grant no. 2004AA32G090).

References

1. G. Velu, D. Remiens, J. Eur. Ceram. Soc. **19**, 2005 (1999)
2. H.Y. Cheung, F.F. Hau, J. Wang, K.H. Wong, Ferroelectrics **260**, 563 (2001)
3. R.C. Buchanan, J. Huang, J. Eur. Ceram. Soc. **19**, 1467 (1999)
4. E. Fribourg-Blanc, E. Cattan, D. Remiens, E. Defay, Solid-State Electron **47**, 1631 (2003)
5. Y.L. Lu, G.H. Jin, M. Cronin-Golomb, S.W. Liu, H. Jiang, F.L. Wang, J. Zhao, S.Q. Wang, A.J. Drehman, Appl. Phys. Lett. **72**, 2927 (1998)
6. H.Q. Fan, G.T. Park, J.J. Choi, H.E. Kim, J. Am. Ceram. Soc. **85**, 2001 (2002)
7. W. Gong, J.F. Li, X.C. Chu, L.T. Li, J. Am. Ceram. Soc. **87**, 1031 (2004)
8. H. Suzuki, T. Koizumi, Y. Kondo, S. Kaneko, J. Eur. Ceram. Soc. **19**, 1397 (1999)
9. Z. Kighelman, D. Damjanovic, N. Setter, J. Appl. Phys. **89**, 1393 (2001)
10. W. Gong, J.F. Li, X.C. Chu, Z.L. Gui, L.T. Li, J. Eur. Ceram. Soc. **24**, 2977 (2004)
11. M. Es-Souni, A. Piorra, C.H. Solterbeck, M. Abed, Mater. Sci. Eng. B Solid-State Mater. Adv. Technol. **86**, 237 (2001)
12. I. Boerasu, L. Pintilie, M. Pereira, M.I. Vasilevskiy, M.J.M. Gomes, J. Appl. Phys. **93**, 4776 (2003)
13. C. Sudhama, A.C. Campbell, P.D. Maniar, R.E. Jones, R. Moazzami, C.J. Mogab, J.C. Lee, J. Appl. Phys. **75**, 1014 (1994)